LEVEL $\mathbb{II}$

LASER ANNEALING OF ION
IMPLANTED GALLIUM ARSENIDE

THESIS

AFIT/GEO/PH/78D-3

ROBERT S. MASON
2 Lt   USAF
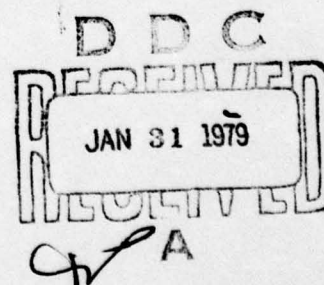
79 01 30 159

AFIT/GEO/PH/78D-3

LASER ANNEALING OF ION
IMPLANTED GALLIUM ARSENIDE

THESIS   Master's thesis

Presented to the Faculty of the School of Engineering

of the Air Force Institute of Technology

Air Training Command   68 p

in Partial Fulfillment of the

Requirements for the Degree of

Master of Science

by

Robert S. Mason

2 Lt   USAF

Graduate Electro-optics

December 1978

PREFACE

Despite results short of those expected, the work done on this thesis was interesting and rewarding for two reasons; (1) the topic was contemporary, allowing me to do essentially "state of the art" work with laser annealing and to observe phenomenon with ion-implanted GaAs which few researchers have seen, and (2) the people I worked with were highly interested in my research. My thanks go especially to my advisor, Dr. Theodore Luke, whose own excitement with and interest in this thesis motivated my work. Thanks also to Dr. Robert Hengehold for discussion and analysis of cathodoluminescence spectra, and to Quiesup Kim of the Air Force Avionics Laboratory for ellipsometry and electrical measurements.

This preface would not be complete without a special thank-you to Marianne, whose daily support, even from 600 miles away, was a major stimulant for the work done during this thesis.

Robert S. Mason

TABLE OF CONTENTS

LIST OF FIGURES AND TABLES

ABSTRACT

Ion implanted GaAs, irradiated by a Q-switched ruby laser, is examined primarily by cathodoluminescence, as well as ellipsometry and electrical measurements, to evaluate the quality of laser anneal. Weak cathodoluminescence spectra from laser irradiated samples indicate far less radiative centers than in thermally annealed samples. Emitted radiation from existing centers is attenuated by the formation of a surface layer on GaAs during exposure to the ruby laser, resulting in spectra which is slightly weaker than spectra representative of the material's condition. This attenuating layer occurs in both virgin and implanted GaAs exposed to the ruby laser.

Ion implanted Si, exposed to the same Q-switched ruby laser, is examined by Rutherford backscattering and indicates a return to crystallinity of the implant layer.

LASER ANNEALING OF
ION IMPLANTED GALLIUM ARSENIDE

I. <u>INTRODUCTION</u>

The material Gallium Arsenide (GaAs) has found many
useful applications, several of which are of interest to the
Air Force today. These include optical detectors, medium
power microwave sources, gigahertz field effect devices,
diode lasers, and solar cells. The result has been a demand
for the formation of better n-type layers, p-type layers,
or p-n junctions within the GaAs, depending upon what
electrical characteristics are necessary for the specific
application. The electrical properties of these layers or
junctions are determined primarily by the concentration and
distribution of dopants introduced into the host material.
These dopants are added to the semiconductor by several
methods, the most popular being: (1) growing the semiconductor
crystal from a mixture containing a specified amount of
the desired impurity, (2) thermally diffusing the desired
impurity into the semiconductor crystal lattice, (3) alloying
the desired impurity into the semiconductor substrate,
(4) introducing the dopant into the semiconductor during
epitaxial growth of the host material upon the existing
crystal lattice, and (5) ion implantation.

Ion implantation is a tool which is particularly attractive
for GaAs, since this semiconductor decomposes at the temperatures
necessary for epitaxy or diffusion. In the implantation

process ions generated in a source are accelerated through
a voltage potential (usually between 20 and 400 keV) and directed
onto the surface of the semiconductor substrate. When a
semiconductor crystal lattice is bombarded by a beam of
high energy ions, the host material will lose some of its
atoms by sputtering, but the lattice will also retain a
significant fraction of the incident ions. The ions remaining
in the semiconductor crystal are said to have been implanted.
The depth to which the ions are implanted depends, in part,
on the incident ion energy. The total number of implanted
ions is a function of the ion beam current, the exposure or
implant time, and the temperature of the host during implantation.

There are advantages, and also disadvantages, of the
implantation process. Some significant advantages are:
(1) impurity concentrations in excess of solubility limits
in certain host materials can be introduced, (2) impurity
distributions much different from other techniques can be
obtained, (3) very shallow, uniform layers can be produced
which allow device fabrication over a very small area; this is
ideal for such applications as integrated circuits, and (4) the
concentration of the dopant can be controlled more exactly.
Some important disadvantages are: (1) the ion bombardment damages
the orderly crystal structure arrangement of the host material
and may leave such defects as dislocations and dislocation loops,
stacking faults, point defect clusters, and subgrain boundaries
(Ref. 16, 28, and 36), (2) few ions take up substitutional
lattice sites in the host, as desired, and, (3) the
resultant implant layer is often left polycrystalline

2

or completely amorphous. The effect of these disadvantages is to limit the number of electron donors and acceptors and decrease carrier mobility, reducing the effectiveness of the implant.

Ion implantation is always followed by thermal annealing as a means of alleviating some of the disadvantages due to the implant. The thermal anneal involves placing the sample in an oven and heating it to a high temperature for usually less than an hour. However, this process is time consuming, and it has its own inherent disadvantages. For instance, the thermal anneal heats the entire sample, sometimes resulting in the decomposition of the host material even in non-implant areas. Short of decomposition, the thermal anneal may degrade the resultant electrical properties by allowing the implant to diffuse throughout the sample; a good junction or dopant layer depends on a localized concentration of dopant. Also, dislocation loops and stacking faults are little affected by this method (Refs. 25, 36, and 38).

Ideally, if the heating were restricted to the implant area only, then a much more localized anneal could be realized. Recent work with annealing by laser beams has made this concept possible.

Laser annealing was first carried out by the Russians in 1974, and published Soviet work (Refs. 2, 4, 20-29, and 37) has generated interest in the United States. Much of the present research in this country is being done at Oak Ridge National Laboratories in Tennessee (Refs. 30, 36, 47, 49, and 50),

3

Stanford Laboratories in California (Refs. 13 and 14), and Bell Labs in New Jersey (Refs. 8, 17, and 33). Thus far, the great majority of the work has been with ion implanted silicon (Si), although a few articles can be found on laser annealing of GaAs (Refs. 4, 7, 17, 20, 21, 24, and 37).

Reported advantages of laser annealing include: (1) greater electrical activity of the impurity than with thermal annealing (see, for example, Ref. 25 or 47), (2) less residual damage than with thermal annealing; specifically, elimination of dislocation loops and stacking faults (see, for example, Ref. 36 or 49), (3) exceeding the solid solubility limit of the dopant within the host material (see, for example, Ref. 17 or 35; in Ref. 17, Golovchenko and Venkatesan claim to exceed the solid solubility limit of tellurium (Te) in GaAs by an order of magnitude), and (4) less diffusion of the dopant, resulting in a narrower depth distribution than possible with thermal annealing (see, for example, Ref. 25; also, see Ref. 49, where it is reported that laser annealed samples have a wider dopant distribution than thermally annealed samples: some theories for this behavior will be presented later). In addition, some authors have tested doped semiconductor devices created by ion implantation and subsequent laser annealing. For example, Golovchenko and Venkatesan (Ref. 17) examined the diode formed by implanting p-type GaAs with zinc (Zn) ions and annealing by laser. They recorded forward

4

resistance and breakdown voltage comparable to thermally annealed samples, and they implied that refined laser annealing techniques might result in better characteristics.

The purpose of this thesis is to establish the correct parameters for annealing of GaAs by a Q-switched ruby laser, based on cathodoluminescence analysis. Samples to be examined will include Te-doped and germanium (Ge) - doped GaAs. Other methods of analysis will be done by supporting laboratories at Wright-Patterson Air Force Base. The results will be compared to published work. Also, laser irradiated Si samples will be examined as a precedent to research on GaAs, since more information is available about Si.

II. BACKGROUND MATERIAL

Ion Implantation and Thermal Annealing of GaAs

A very appealing aspect of ion implantation is the degree of control over the parameters of the implant. One of the most important is implant depth. As mentioned previously, this depth depends, to a large extent, on the implant beam energy. Table I shows calculated implant depths, with standard deviations, for various ions implanted in GaAs, based on LSS theory. The two implant energies shown serve as good upper and lower bounds for typical implants. The standard deviation represents a distribution nearly gaussian in form, with the peak of the distribution at the noted implant depth. Of interest, in addition to the dopant distribution, is the degree of damage of the implant layer. The damage is dependent on: (1) ion mass, (2) ion fluence, (3) the temperature of the host during implantation, and (4) the implant beam flux.

To remove the damage of the implant layer by thermal anneal, GaAs must be "capped" with a protective coating, such as silicon nitride (Si_3N_4) or silicon dioxide (SiO_2) (Ref. 9). Significant decomposition of the material occurs at about 600°C (Ref. 46), while temperatures necessary for thermal anneal exceed 800°C. The mechanisms of thermal annealing are different in various materials. A good comparison is Si and GaAs, not only because the mechanisms are different for these materials, but also because most of the information about laser anneal to be presented later is based on research with Si only.

6

Major differences in thermal annealing of Si and GaAs
are (Ref. 12): (1) Si anneals over a narrower temperature
interval than GaAs, (2) there is a preferred substrate
orientation for recrystallization in Si, but this is not
true for GaAs, and (3) there is always a greater degree of disorder
in GaAs than in Si after thermal annealing under the same
conditions.

Another difference in the two materials is that Si exhibits
better electrical behavior for implantation at room temperature
followed by thermal annealing, whereas hot substrate implantation
followed by thermal annealing is necessary for high electrical
activity in GaAs (Ref. 12).

Table I. Projected implantation depth (R_p)
and standard deviation (ΔR_p) for ions implanted
in GaAs. (From Donnelly, Ref. 9, p. 167.)

| | 20 keV | | 400 keV | |
Ion	R_p (μm)	ΔR_p (μm)	R_p (μm)	ΔR_p (μm)
p-type				
Be	0·062	0·041	1·092	0·205
Mg	0·022	0·014	0·453	0·127
Zn	0·011	0·006	0·157	0·064
Cd	0·009	0·004	0·098	0·040
n-type				
Si	0·018	0·012	0·351	0·121
S	0·017	0·011	0·307	0·110
Se	0·011	0·005	0·137	0·056
Sn	0·009	0·004	0·095	0·038
Te	0·009	0·004	0·092	0·036

Laser Interaction with GaAs

The absorption coefficient (α) for pure GaAs is 2×10^4 cm^{-1} at the ruby wavelength, $\lambda = 6943\text{Å}$ (Ref.20). After implantation, the absorption will increase, due to damage in the implant layer, but the degree of change is unknown. The effect of the implantation at the air-implant layer interface, as well as the implant layer-substrate interface, and hence on the refractive index at these boundaries, is also in question. These parameters need to be established to determine the criteria for selection of a laser to be used for annealing of GaAs. First of all, one must know how much laser energy incident on the surface reaches the implant layer through the interface and, secondly, how much of this energy is absorbed by that layer.

For purposes of discussion, and as a lower limit, one can assume an absorption coefficient at 6943Å ($\alpha_{.69um}$) for a polycrystalline or amorphous GaAs layer as being the same as for the pure material. Using 2×10^4 cm^{-1} for $\alpha_{.69um}$, ruby laser radiation incident on an ion implanted GaAs layer would be down to roughly 40% of its surface value at .5um from the interface, assuming an exponential decay. Therefore, shallow implant profiles for various ions implanted in GaAs at 20 keV implantation energy, given in Table I, mean that the decrease of ruby laser energy over the implant layers in these cases would be small, for the assumed absorption coefficient. On the other hand, for implants of 400 keV implantation energy in GaAs, also given in Table I, a substantial decrease of laser energy occurs within the implant layers. This is further

complicated by the fact that higher implant energies cause a greater degree of damage, increasing the absorption coefficient and further enhancing the decay of incident laser energy. Since a higher implant energy results in a deeper implant profile and increased absorption coefficient, laser energy incident on such an implant layer might decay to a small fraction of its surface value by the time it reaches the implant layer-substrate boundary. The determining factor would be how much the absorption coefficient increases after ion implantation.

The amount of laser energy absorption in a material also depends on the type of laser used. Figure 1 shows the relationship between α and laser photon energy $h\nu$ for GaAs. Ge and Si are shown for comparison. The energy below which the absorption coefficient is ≥ 1 for a given material is called the fundamental absorption edge, or energy gap, of that material. Figure 1 indicates that α increases drastically as soon as the photon energy corresponding to the energy gap is exceeded. For example, the photon energy of the ruby laser is 1.79eV, far exceeding the energy gap of GaAs, 1.43eV, and resulting in a large absorption coefficient at the ruby wavelength for this material.

As a comparison, another common laser, neodymium - YAG (Nd-YAG), or neodymium-glass (Nd-glass) with λ = 1.06um, has photon energy of 1.17eV, below the GaAs energy gap. This means that a 100% pure GaAs material would be nearly transparent for a neodymium laser. All GaAs semiconductors have some impurities, however, as well as defects in crystal structure.

9

In fact, some GaAs used for ion implantation is of the semiinsulating type, doped with chromium (Cr). These impurities and imperfections will absorb neodymium laser light (Ref. 40). It is reasonable to assume, therefore, that ion implanted GaAs will absorb neodymium in areas damaged by ion implantation. The absorption coefficient at 1.06um ($\alpha_{1.06um}$) will be proportional to the damage. Consequently, for large degrees of damage, $\alpha_{1.06um}$ will change considerably more than $\alpha_{.69um}$, when compared to the virgin material. The overall amount of absorption in even a heavily damaged implant layer of GaAs,
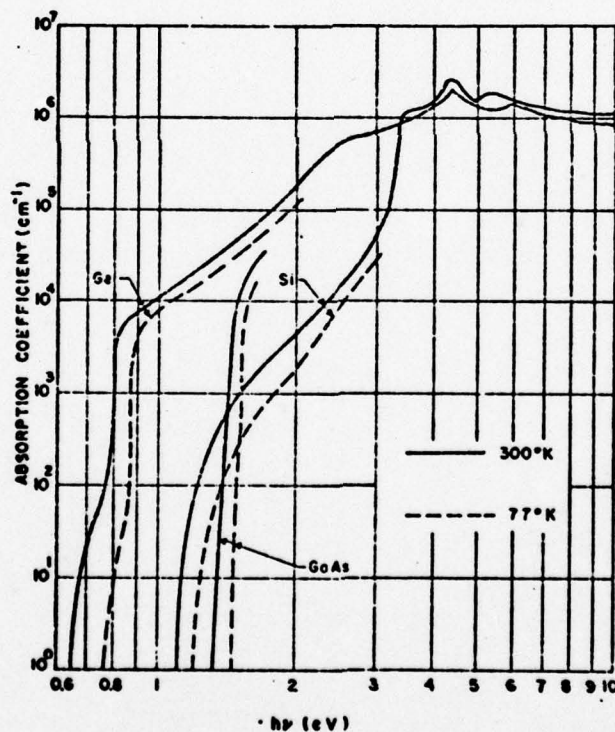

Figure 1. Absorption coefficient dependence on photon energy. Energy gaps for Ge, Si, and GaAs at 300°K are .66, 1.12, and 1.43eV, respectively. (From Sze, Ref. 42, p. 54)

however, will be less for neodymium than for ruby, since only the defects and imperfections are absorbing at 1.06um, while at 6943Å both these and the bulk, or undamaged, material are absorbing the laser energy.

The photon energy for Nd-YAG, or Nd-glass, is only slightly above the fundamental absorption edge of Si, 1.12eV, with the result that $\alpha_{1.06um}$ for pure Si is not much greater than $\alpha_{1.06um}$ for pure GaAs. At the same time, $\alpha_{.69um}$ is large for both materials. Therefore, the effect of implantation on α for Si and GaAs should be similar at the neodymium and ruby wavelengths, assuming defects in GaAs absorb roughly the same as defects in Si at both wavelengths.

Khaibullin, et. al. (Ref. 25), found that a slightly disordered Si layer has $\alpha_{.69um} = 4 \times 10^3 cm^{-1}$ and $\alpha_{1.06um} = 20cm^{-1}$, while an amorphous Si layer has $\alpha_{.69um} = 4 \times 10^4 cm^{-1}$ and $\alpha_{1.06um} = (3-6) \times 10^3 cm^{-1}$. Note that $\alpha_{.69um}$ in the amorphous layer has increased by less than 1000% over $\alpha_{.69um}$ for the slightly disordered layer, while $\alpha_{1.06um}$ has changed by more than 10,000% for the same two layers. As with GaAs, the reason is that $\alpha_{1.06um}$ for an amorphous, polycrystalline, or crystalline Si layer is determined primarily by the defects present in that layer; the absorption by the bulk material is small compared to the absorption by defects at the neodymium wavelength. Note also that $\alpha_{.69um}$ is always greater than $\alpha_{1.06um}$, regardless of the layer condition. Again, as with GaAs, this is because $\alpha_{.69um}$ is greater than $\alpha_{1.06um}$ for pure Si, and the bulk material present, even in heavily damaged

11

Si layers, will absorb ruby laser radiation more than neodymium laser radiation.

In every material, absorption due to the bulk exists as well as an absorption due to defects within the bulk. These two factors determine the overall absorption and, hence, the total absorption coefficient. For the case of GaAs and Si, damage resulting from ion implantation has nearly the same effect in both materials on total absorption at the neodymium wavelength. Defects determine $\alpha_{1.06um}$ in GaAs to a slightly greater extent than in Si because pure GaAs absorbs less than pure Si at $\lambda = 1.06um$. Therefore, the percent change in $\alpha_{1.06um}$ between crystalline and amorphous layers ($\Delta\alpha_{1.06um}$) in GaAs will always be greater than in Si. $\Delta\alpha_{1.06um}$ in Si will, however, approach $\Delta\alpha_{1.06um}$ in GaAs as the damage in both materials increases.

Again for the case of GaAs and Si, damage resulting from ion implantation has nearly the same effect in both materials on total absorption at the ruby wavelength as well. Defects determine $\alpha_{.69um}$ in GaAs to a slightly lesser extent than in Si because pure GaAs absorbs more than pure Si at $\lambda = .69um$. Therefore, the percent change in $\alpha_{.69um}$ between crystalline and ampophous layers ($\Delta\alpha_{.69um}$) in GaAs will always be less than in Si. $\Delta\alpha_{.69um}$ in GaAs will, however, approach $\Delta\alpha_{.69um}$ in Si as the damage in both materials increases.

Laser Annealing

The concept of what "annealing" of a substrate means has not been clearly defined in the published work on laser anneal; obviously, there are different degrees of anneal. For instance, "slightly" annealed means the characteristics of the laser irradiated sample are considered little better than that of an implanted sample which is neither heated or exposed to laser light. Most authors use the term "laser annealing" to mean an effect which produces characteristics in a sample comparable to, or better than, thermal annealing; characteristics such as elimination of defects, substitutionality in the crystal lattice of the host by implanted ions, increased carrier mobility, increased conductivity, and/or return of the amorphous layer due to ion implantation to a crystalline state. These improved characteristics are verified by different types of analysis of laser irradiated, implanted material which include: reflection; both visible and infared (see, for example, Ref. 29 or 39), high energy electron diffraction (see, for example, Ref. 10 or 44), Rutherford backscattering (see, for example, Ref. 11 or 31), infared light transmission (see, for example, Ref. 4), Hall effect (see, for example, Ref. 20 or 24), resistivity (see, for example, Ref. 17 or 21), microscopic photography (see, for example, Ref. 20 or 25), and secondary ion mass spectroscopy (see, for example, Ref. 13 or 49).

There are different techniques for laser anneal being pursued today. Suggestions on technique break down into two basic trends of thought, with divergent approaches in each.

These are liquid-phase epitaxial regrowth and solid-phase epitaxial regrowth. Liquid-phase epitaxial regrowth involves raising the temperature of the material above its melting point. Pulsed lasers have been used almost exclusively for this method, due to their high energy output. The concept is as follows (Ref. 47): during the laser pulse, the surface temperature rises past the point of melt. The "melt front" moves inward and reaches its maximum depth in slightly more time than the duration of the pulse. As the material cools down, the region that was melted recrystallizes, with the implanted ions in substitutional lattice sites. A recognized consequence of liquid-phase epitaxy is a dopant profile which is wider than the corresponding profile in a thermally annealed sample (Ref. 38). This is the result of diffusive redistribution due to thermal effects and possibly ionization enhanced diffusion (Ref. 5). The width of the dopant profile is determined by incident laser energy, pulse duration time, and the mobility of the dopant in the host material. Figure 2 shows dopant profiles of boron (B) in Si after irradiation at several laser energies. Higher energies result in deeper dopant profiles, as shown.

Rimini, et. al. (Ref. 37), somewhat verified the liquid-phase epitaxy concept by showing that the difference in anneal thresholds in Si and GaAs implanted under the same conditions was approximately the same as the difference in their melting points. White, et. al. (Ref. 47), found that the surface of Si melted for the 50 nanosecond pulse of a ruby laser whose intensity was greater than 1.1 joules/cm^2, while annealing
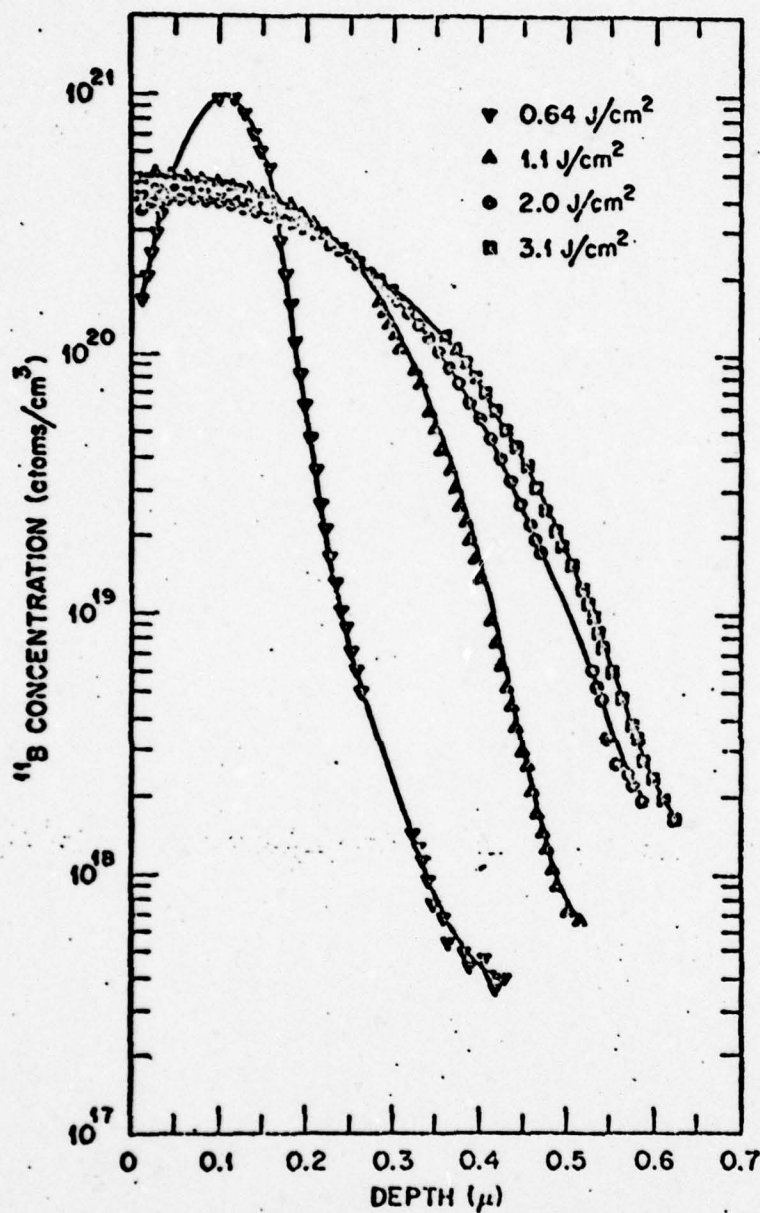
14

Figure 2. Concentration profiles of B in Si after laser annealing. Higher laser energies caused wider profiles, as shown. (From White, et. al., Ref. 47.)

did not take place until the intensity was 1.3 joules/cm^2,
for a B-implanted sample. Baeri, et. al. (Ref. 3) have done
detailed studies with the melt area of Si due to laser light to
support laser annealing work based on liquid-phase epitaxy.
Based on Rutherford backscattering analysis, they claim that
the entire amorphous layer must become liquid before recrystallization
can occur. Figure 3 is from their theoretical calculations and
provides a graphical method of predicting the melted area of
amorphous Si. If they are correct about the melting requirement,
this is a reliable way of selecting the necessary anneal energy
for an implanted layer, based on implant depth.

Solid-phase epitaxial regrowth theory is less widespread
than the liquid-phase epitaxy concept. The main proponets of
this technique are Stanford Laboratories, although Bell Labs
have shown heavy interest in both approaches. Bell is using
an argon-ion laser to raise the
temperature of Si to between 900°C
and 1300°C, below the 1400°C melting
point. Krypton, as well as argon,
lasers have been used most for this
method. They are operated continuous
wave (CW) and often in conjunction with
scanning apparatus. The main advantage
of this type of annealing is a dopant
profile which is narrower than that
possible with thermal annealing (Ref. 38),
since less diffusion of the implant
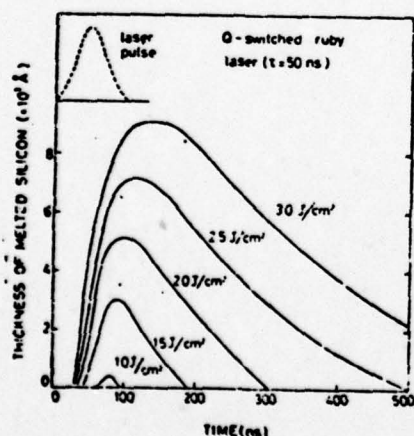takes place during laser annealing

Figure 3. Calculated
melt depth for amorphous
Si. (From Baeri, et.
al., Ref. 3, p. 138.)

16

by solid-phase epitaxy. Even though thermal anneal temperature and laser anneal temperature are comparable in this case, the time during which the material is subjected to elevated temperature is much shorter for laser annealing, thereby allowing less time for diffusion. Figure 4 shows the dopant profile of an arsenic (As) - implanted Si sample which has been laser and thermally annealed, as well as the calculated LSS profile. Laser annealing for this case was by solid-phase epitaxial regrowth, taking place below the melting point. Suggested benefits of a narrower dopant profile include producing integrated circuits whose device density is an order of magnitude above the best available today (Ref. 38).

Interesting features of pulsed laser annealing, and a stimulant for research in this area, are the athermal effects that have been theorized for very fast laser pulses ($<10^{-7}$ sec) generated by operation in the Q-switched mode. These are: (1) strong ionization, (2) coherent interaction of light with the lattice, (3) shock waves, and (4) the appearance of electric fields in the illuminated layers; in short, anything due to an intense interaction of laser light with the material (Ref. 25). Q-switched lasers have also caused dopants to exceed the solid solubility limit of the host. Khaibullin, et. al. (Ref. 25), suggested that this was due to an extremely fast transition of the amorphous layer to a nonequilibruim, liquid state. Subsequently, there is a rapid solidification of the material, so that the system is "frozen" in this state. They supported the idea by thermally annealing a sample that had been laser annealed and was in an above saturation condition. The result was a return of the dopant concentration to the solid solubility
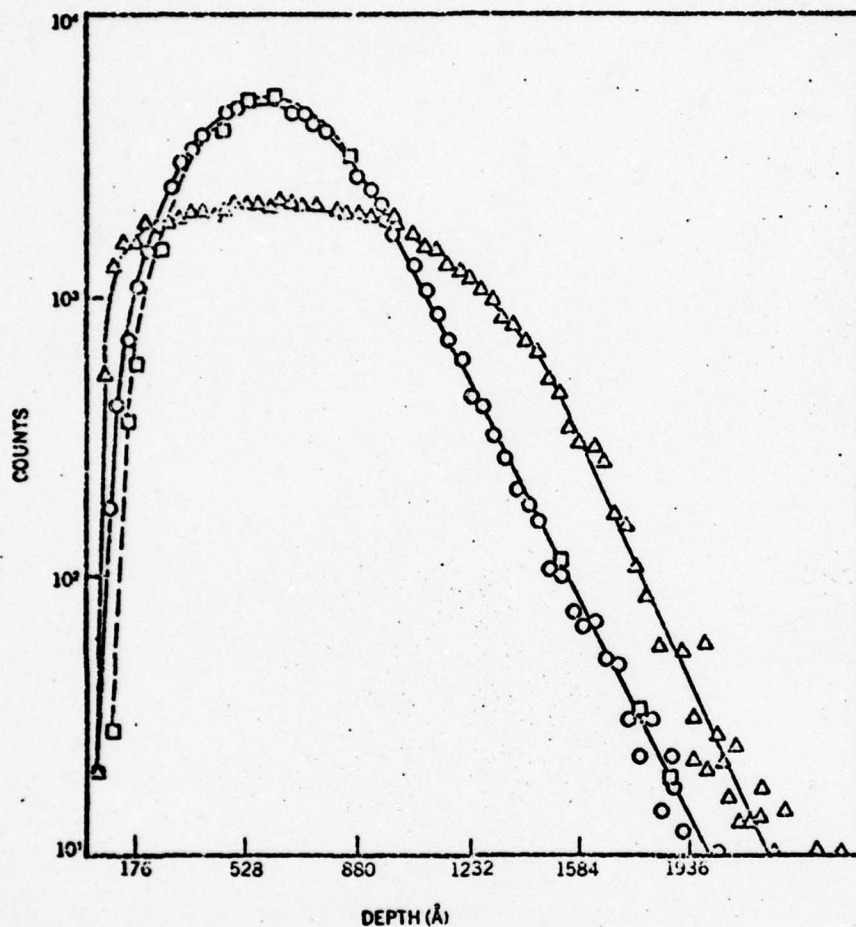
Figure 4. Concentration profiles of As in Si after laser annealing. Δ indicates the thermally annealed profile, o the laser annealed profile, and □ the calculated profile. (From Gat, et. al., Ref. 14, p. 277.)

limit. They based these observations on sheet conductivity measurements.

Researchers who have speculated on athermal effects of Q-switched pulses all agree that while they do exist, they will not be verified without more concentrated research of laser annealing.

A particular advantage of Q-swtiched lasers for GaAs is this extremely quick melting and recrystallization of the implant layer. For uncapped GaAs, As will outdiffuse and leave the surface during thermal anneal. This occurs well below the melting point, so even solid-phase epitaxial regrowth might cause the same effect. Arsenic may be "frozen" in place during a Q-swtiched laser pulse in the same way that implanted ions are in Khaibullin, et. al.'s theory. Smith (Ref. 40) did note that a gallium (Ga) rich layer forms during millisecond pulses from a ruby laser, but that the concentration of Ga decreases substantially for Q-switched pulses of 20 nanoseconds. Perhaps shorter pulses would eliminate this layer altogether.

Establishing a laser energy range for anneal of GaAs has not been done. In fact, conflicting figures in the literature make estimation very difficult. It is not clear whether incident energy or incident peak power is the determining factor in the annealing process; some authors in the published work give energy figures, some state power figures, and still others supply both.

The optimum annealing energy for Si is reported to be below the damage threshold (Ref. 25), damage here being

defined as changes in the surface appearance of the material
such as microcracks, scattered craters, or cavities observable
under a high power microscope. Table II shows incident ruby
laser energy and power figures from the literature for different
implant concentrations and implant energies of Te in GaAs.
The list seems consistent; increased laser energy densities
being required for deeper implants created by higher implant
energies. Yet, the peak power densities corresponding to
these energies almost all exceed what Smith (Refs. 40 and 41)
calls the damage threshold of GaAs; $8MW/cm^2$. Smith did
not specify energy figures, so these cannot be compared.
Reasons for the obvious discrepancy are not apparent.

Khaibullin, et. al. (Ref. 25), made the best attempt at
bracketing the anneal energy for Si with various implants.
They call the anneal threshold the recrystallization threshold,
while the limit beyond which damage occurs in defined as the
light distortion threshold. These thresholds differ for
neodymium and ruby lasers, and the anneal threshold itself
is variable for the neodymium wavelength, depending on implant
parameters. This reverts back to earlier discussion about the
consequences of choosing a laser whose photon energy is close
to or below band gap, as well as considerations of absorption
coefficient for different wavelengths based on the degree
of damage in the implant layer. For ruby, the recrystallization
threshold is given as $\sim 5MW/cm^2$, and the light distortion
threshold as $\sim 35MW/cm^2$. Annealing is reported to occur
within this range, and they define an optimum annealing energy

TABLE II

Q-switched ruby laser energy and power densities for laser anneal of Te-doped GaAs (from published work).

CONCENTRATION Te/cm^2	IMPLANT ENERGY keV	LASER ENERGY DENSITY J/cm^2	LASER POWER DENSITY MW/cm^2
10^{15}	35	.057	1.9
10^{15}	35	--	1-10
10^{15}	40	.2	6.6
10^{16}	50	.29	24
10^{15}	400	1.2-1.4	24-70

21

somewhere between 5 and 35MW/cm^2, although the exact number
is not specified.

Many have verified these laser power figures, but others
show disagreement. Vitali, et. al. (Ref 44), reported that
40-60MW/cm^2 was necessary to anneal an amorphous layer
in pure Si between 2000Å and 4000Å deep. Foti, et. al.
(Ref. 11), used ruby pulses as high as 60MW/cm^2 to anneal
Si doped with 10^{15}Te/cm^2, with an implant energy of 400keV.
There are other conflicting reports. The majority of the
published work is in agreement with Khaibullin, et. al.,
however, and their work is recognized as a significant
contribution to laser annealing of Si. A similar analysis of
various implants in GaAs is essential, but this study has not
yet been done. To bracket the laser anneal energy for GaAs,
one must know the exact effect of ion implantation on this
material in terms of refractive index and absorption coefficient,
for a given wavelength, based on implant type, dose, and depth.
Only then can a reliable prediction of required laser anneal
energy for GaAs be established. Interest in GaAs has increased
in recent years, and it is conceivable that analysis of this
material similar to that done already with Si will occur
in the near future.

There has been some published work comparing laser annealing
of GaAs and Si (Refs. 20, 25, and 37). A noted difference is
that Si requires considerably more incident laser energy to
anneal than does GaAs. The reported laser anneal energies are
not consistent, but those for Si Are generally 50% higher

than for GaAs at the ruby wavelength. This can be attributed, in part, to different absorption coefficients in the two materials at $\lambda = 6943\overset{\circ}{A}$. Also, the laser anneal mechanisms may be different in Si and GaAs, based on contrasting thermal anneal mechanisms observed earlier.

A very important consideration when comparing laser annealing of the two materials is whether GaAs has the same type of energy bracket for laser anneal proposed by Khaibullin, et. al., for Si. If the range of laser energies necessary for annealing is very small for GaAs, this would eliminate certain lasers from being used for this purpose. For instance, reasons were presented earlier for large absorption of laser light in ion implanted semiconductors. It was shown that the possibility existed for incident laser energy to decay to a very small portion of its initial value within the implant layer. This is particularly true for ruby laser energy incident on GaAs samples that have been implanted at high implant energies. The question here is whether the range of energies in an implant layer of GaAs must all fall within the laser anneal bracket. It has been demonstrated that this is not the case with Si; despite high absorption, heat on the surface of an implanted Si sample generated by incident ruby laser energy was transported throughout the implant layer, resulting in a complete anneal (Ref. 3). It is not known whether this can occur in GaAs.

It is conceivable that ruby will not be a feasable laser to use for annealing of GaAs, due to high absorption in this

30

23

material at $\lambda = 6943$Å. For instance, a laser energy density
corresponding to the damage, or light distortion, threshold
for GaAs, incident on an implanted GaAs sample, might quickly
decay and anneal only that portion of the implant layer near
the surface. Raising the incident laser energy to anneal the
entire implant layer would then result in damage near the
surface. The only alternative would be to use a laser whose
absorption coefficient is less in GaAs, such as Nd-YAG or
Nd-glass. However, not enough is known about the mechanism of
laser annealing to determine whether the bulk material must
absorb the laser energy; i.e., whether the photon energy
of the laser must exceed the energy gap of the material.
Therefore, the effectiveness of neodymium for laser annealing
of GaAs is not clear.

Appendix A is a summary of published work on laser annealing
of GaAs.

Analysis

Analysis of laser irradiated, ion implanted GaAs by
cathodoluminescence has not been indicated in the literature.
All published work on laser annealing has dealt strictly
with other types of analysis, which were mentioned earlier.
Luminescence is defined as the electro-magnetic radiation
which occurs when electron-hole pairs recombine radiatively
in a semiconductor. Information about implant layers in ion
implanted material can be obtained by excitation of luminescence.
When the stimulant for this excitation is an electron beam, the
technique is called cathodoluminescence. Luminescence theory
is discussed in detail in Ref. 46.

24

Figure 5 shows luminescence spectra for an unannealed GaAs sample implanted with Te ($10^{13}/cm^2$) at an implant energy of 120 keV. Figure 6 shows luminescence spectra for a thermally annealed GaAs sample, also implanted with $10^{13}Te/cm^2$ at 120 keV implantation energy. The main peak in Figure 6 is due to a Te donor to acceptor transition (Ref. 33), located at $\lambda = 8337.8$nm, or 1.487eV. The peak number of "counts" (electron-hole pairs), designated as relative magnitude on the axis, in this case is 31,600. The main peak in Figure 5 is attributed to a conduction band to zinc impurity transition (Ref. 33), located at $\lambda = 9323.9$nm (1.495eV), while the peak due to Te is negligible. Here, the number of counts in the main peak is 550.

The probe depth of the electron beam is determined by the beam voltage, given in Figures 5 and 6. The signal strength, or number of counts, is determined by the condition of the material and the beam current, also given in the two figures. Both samples in Figures 5 and 6 have been probed at the same depth, but the beam current in the unannealed sample is much larger than the beam current in the annealed sample. Yet, the number of counts is much lower for the unannealed sample, indicating a nearly amorphous implant layer, as would be expected. The thermally annealed smaple shows, by the high number of counts, substantial recrystallization.

Thermally annealed sample spectra can be used to set the standard for samples which are laser annealed; that is, samples irradiated by laser light which show spectra comparable
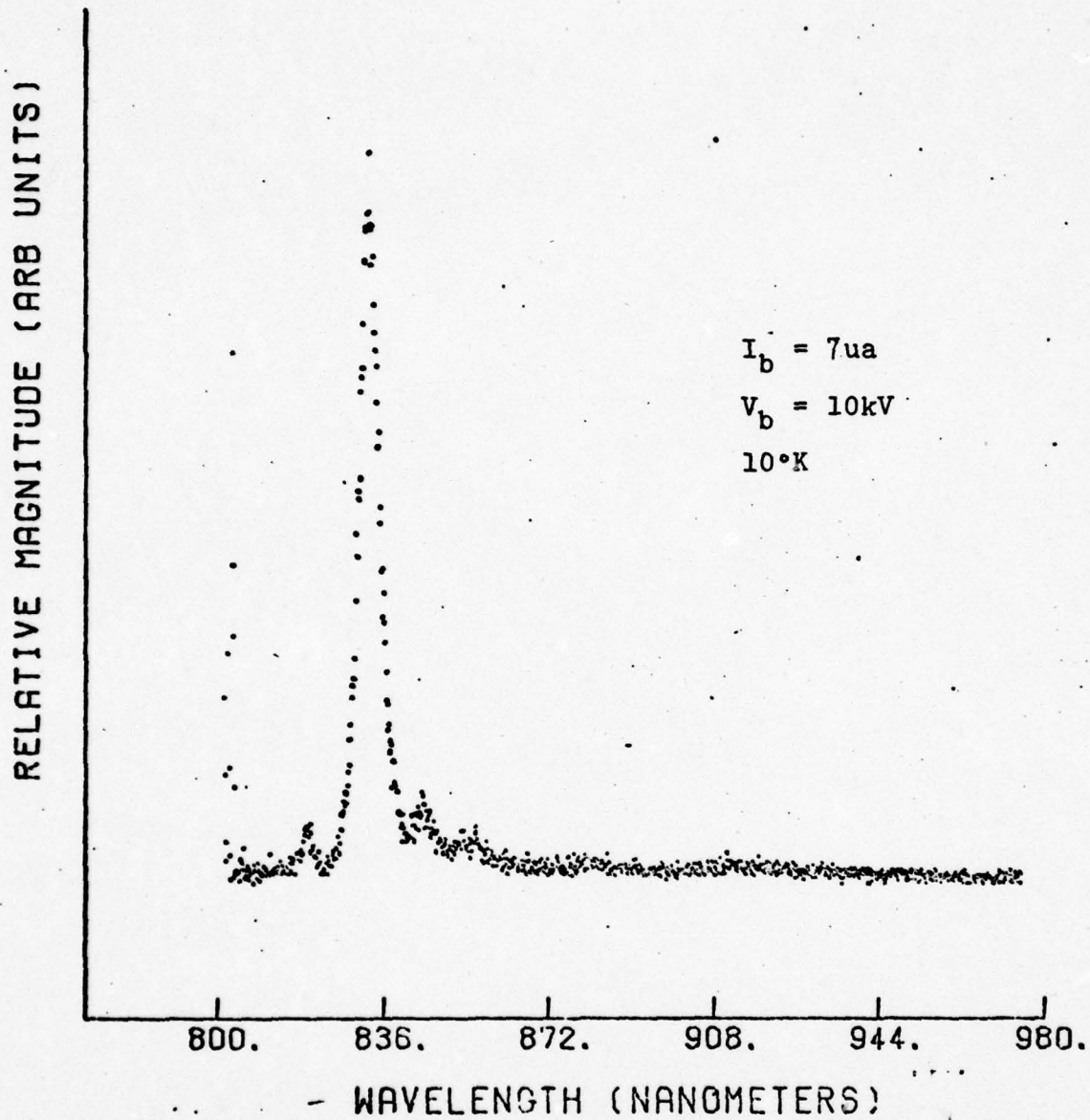
25

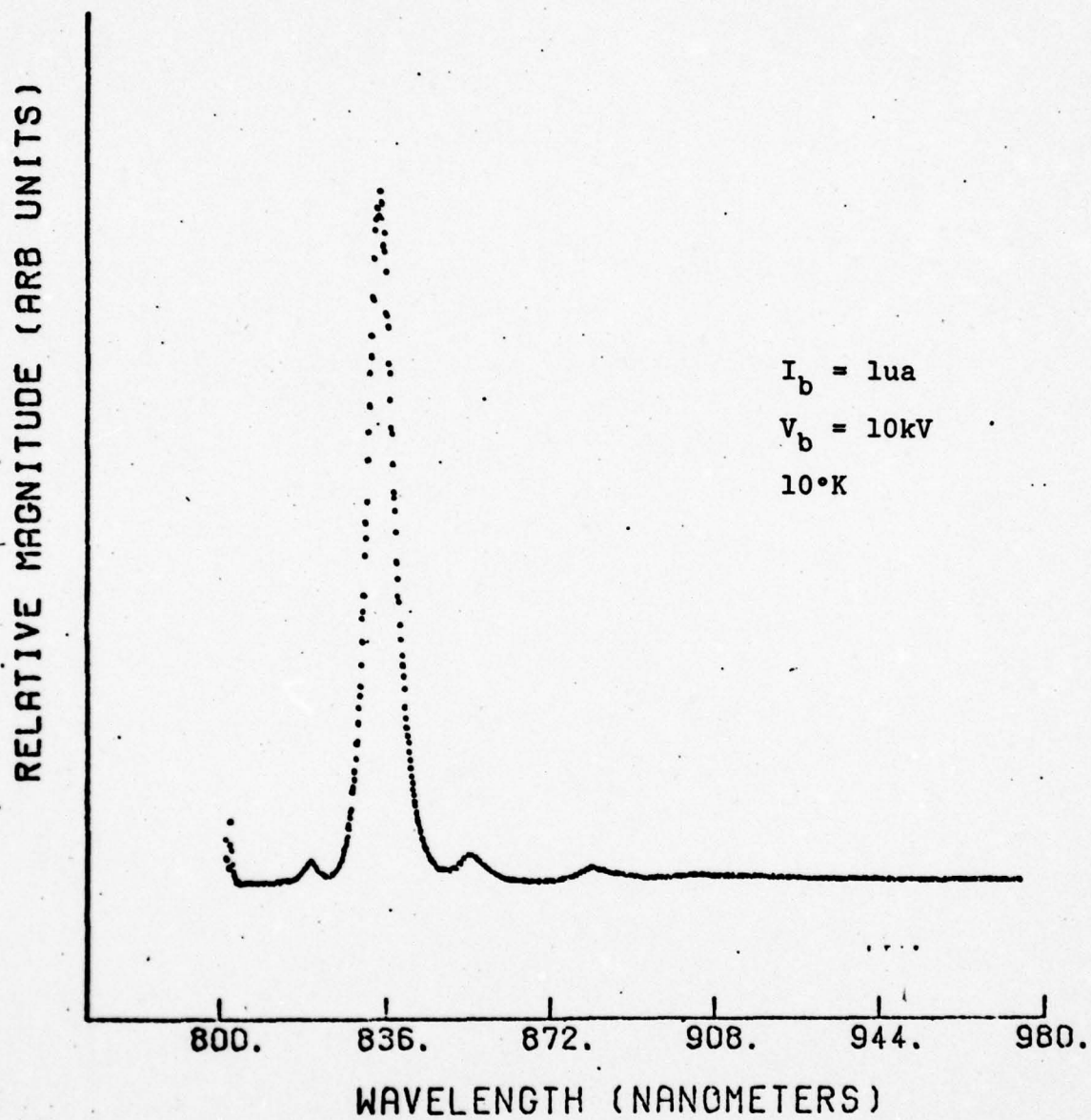Figure 5.   Luminescence of unannealed GaAs implanted with Te.

Figure 6. Luminescence of thermally annealed GaAs implanted with Te.

to thermally annealed material, with the same implant conditions in both, can be considered laser annealed. Any sample spectra which shows only limited improvement over the unannealed spectra can be designated "slightly" or "partially" laser annealed, based on the degree of improvement of the implant layer.

For a detailed discussion of cathodoluminescence spectra of unannealed, thermally annealed, and laser irradiated, Te-Implanted GaAs, see Ref. 33. Ref. 45 has a detailed discussion of cathodoluminescence spectra of unannealed, thermally annealed, and laser irradiated, Ge-implanted GaAs, and it also contains information about spectra from virgin GaAs samples exposed to ruby laser radiation.

Additional analysis of some laser irradiated, ion implanted GaAs samples by laboratories at Wright-Patterson Air Force Base included ellipsometry, Hall effect, and resistivity. Ellipsometry directly measrues a quantity called the extinction coefficient, which is proprotional to the absorption. A decrease in extinction coefficient would indicate anneal since the same decrease in absorption had occurred. Any increased electrical activity would also indicate that some annealing had taken place. Rutherford backscattering, done at the University of Salford, England, for Si samples, would indicate anneal by showing a return to crystalline structure in the implant layer.

III. EXPERIMENT

Laser and Related Equipment

The laser used for this experiment was the Holobeam
Series 300, with a ruby rod 3/8" in diameter and 3" long
pumped by a Xenon-filled arc discharge lamp. This laser can
use neodymium or ruby rods interchangably in the laser head.
Ruby was selected over neodymium based on the assumption that
the laser photon energy must exceed the energy gap of the
material for annealing to occur. Even if neodymium can anneal
GaAs, it was shown earlier that the anneal threshold in
GaAs samples with varying implant conditions will change less
for ruby than for neodymium. This would facilitate the
experimental work. It was assumed that high absorption in the
GaAs at the ruby wavelength would not prevent an effective
anneal, based on previous discussion on absorption.

The Holobeam Series 300 laser can be operated normal mode,
in which case lasing lasts for approximately .7 msec; or, it
can be oeprated in the Q-switched mode, in which case the
pulse duration is between 15 and 25 nanoseconds. Q-switching
is accomplished by a Pockels Cell and Brewster angle polarizer.
The laser head was kept at a constant temperature by a water
cooling unit. Remote stations were used for flash lamp firing
and for setting the Pockels Cell voltage and delay time.
The range of possible values for these parameters were:

        PUMP VOLTAGE 0-5 kV
        POCKELS CELL VOLTAGE 0-10 kV
        POCKELS CELL DELAY TIME 0-3 msec

29

The optimum settings for the Q-switch were found to be:

POCKELS CELL VOLTAGE 8.8 kV
POCKELS CELL DELAY TIME .97 msec

The minimum pump voltage for lasing was variable due to condition of the laser head and cavity alignment. The upper limit on output is given by Holobeam specifications as $200MW/cm^2$, beyond which damage to the ruby rod may result.

The laser cavity was aligned with a Davidson #D657 auto-collimator, and a Spectra Physics #132 helium-neon (HeNe) laser was used for purposes of aiming the ruby laser beam at a designated spot.

Energy measurements were taken with a Quantronix 504 energy/power meter in conjunction with a Quantronix 501 energy receiver. The energy readings were calibrated against a TRG Control Data Corporation 108 thermopile, whose response was 56 microvolts/joule. It was found that the Quantronix meter/receiver combination read $83\frac{1}{3}\%$ of the incident laser energy for an output of approximately 2 joules.

The Quantronix receiver was equipped with a built-in Hewlett-Packard 4220 fast photodiode (2 nanosecond rise time). The diode, biased by a DC voltage of 15-25 volts, was used to monitor the width of the laser pulse. Its output was connected to a Tektronix 7633 oscilloscope with a 7A19 series plug-in amplifier (3.5 nanosecond rise time). This amplifier has an input resistance of 50 Ω and an input capacitance of 200pf, with a minimum time scale sensitivity of 5 nanoseconds/division. Given the fast rise times of both the detector and scope, the pulse width from the laser

30

could be estimated accurately from the scope display, even down to its expected minimum of 15 nanoseconds. Figure 7a is a picture of the Q-switched pulse for a cavity length of 45.7 cm, and figure 7b is a picture of the pulse for a larger cavity of 74.9 cm. The pulse width at half maximum (PWHM) is consistent with the equation for pulse width given by Yariv (Ref. 48; 137);

$$\tau \cong \frac{n\ell}{C(1-R)} \tag{1}$$

where

τ = pulse width

n = 1,2,3...

C = speed of light

(1-R) = cavity losses

ℓ = cavity length

which indicates that cavity length and the PWHM are directly proportional.

Optics: Laser Beam Detection and Control

It was found that changing the pump voltage to vary output energy resulted in a changing pulse width as well. Therefore, a calcite Glan-Foucault polarizer, mounted on a rotatable housing, was used at the output of the laser for variable energy with constant pulse width. Since the output of a Q-switched ruby laser is horizontally polarized, one could either increase or decrease energy incident on a given sample

(a)

(b)

Figure 7. Q-switched ruby laser pulses. The PWHM are
(a) 16 nanoseconds and (b) 24 nanoseconds.

simply by adjusting the split calcite crystal to the proper inclination. Maximum transmission through this poloarizer was found to be ~80%, while the minimum setting gave no detectable output.

The need for a homogeneous laser beam over the area of the samples to be irradiated was necessary for successful annealing. If a beam with sufficient energy to anneal contained any "hot spots" which exceeded the damage threshold, the quality of the laser anneal would be affected. In trying to obtain a homogeneous beam over a limited area, two basic unknowns were considered; (1) a method to accurately display the beam profile, and (2) the optics needed to produce a homogeneous beam area.

Photographic film, mounted and placed in the path of the laser beam past the output mirror, was used to detect the beam profile. The best results were obtained with Polaroid type 47 black and white film. A problem with this approach, however, was that intense heating of the film material at high energy outputs from the laser resulted in an inaccurate profile due to thermal effects in the film chemicals. It was suggested in private correspondence with Holobeam Corporation and Oak Ridge National Laboratories that the laser output be decreased in increments until no impression was left on the film. The resultant profile left by the energy one step above this would be an accurate picture of the beam structure.

The beam profile showed non-gaussian structure, indicating the existence of several transverse modes. This demanded the use of some type of optics to produce the required homogeneous beam area. There are many approaches used to homogenize a laser beam in the published work on laser anneal. While some authors do not specify any optics, others have used a diverging lens (Refs. 4 and 20), a focusing, converging lens (Refs. 8 and 10), and some combination of collimator, glass diffuser, and/or focusing lens (Refs. 17, 18, 25, 29, 39, and 43). In addition, the scanning apparatus mentioned earlier has been used as an alternative to a large homogeneous beam to give an even energy distribution over the area of the sample (Refs. 8, 13, 14, and 21).

Of all the methods tested, the best arrangement was found to be a glass diffuser, which was ground on both sides, used in conjunction with a 4mm diameter tapered aperture. The distance from diffuser to sample was varied and resulted in a trade-off: as the distance was increased, diffusion greatly improved, while usable energy declined; moving the ground glass closer to the aperture increased usable energy at the expense of non-homogeneity in the beam profile. Attempts at focusing the beam into the diffuser to obtain a higher energy density over a small area without affecting beam homogeneity resulted in damage to the ground glass and loss of reproducibility. The optimum arrangement is shown in Figure 8. The distance a is variable depending upon required energy output, with the homogeneity of the beam over the aperture declining for
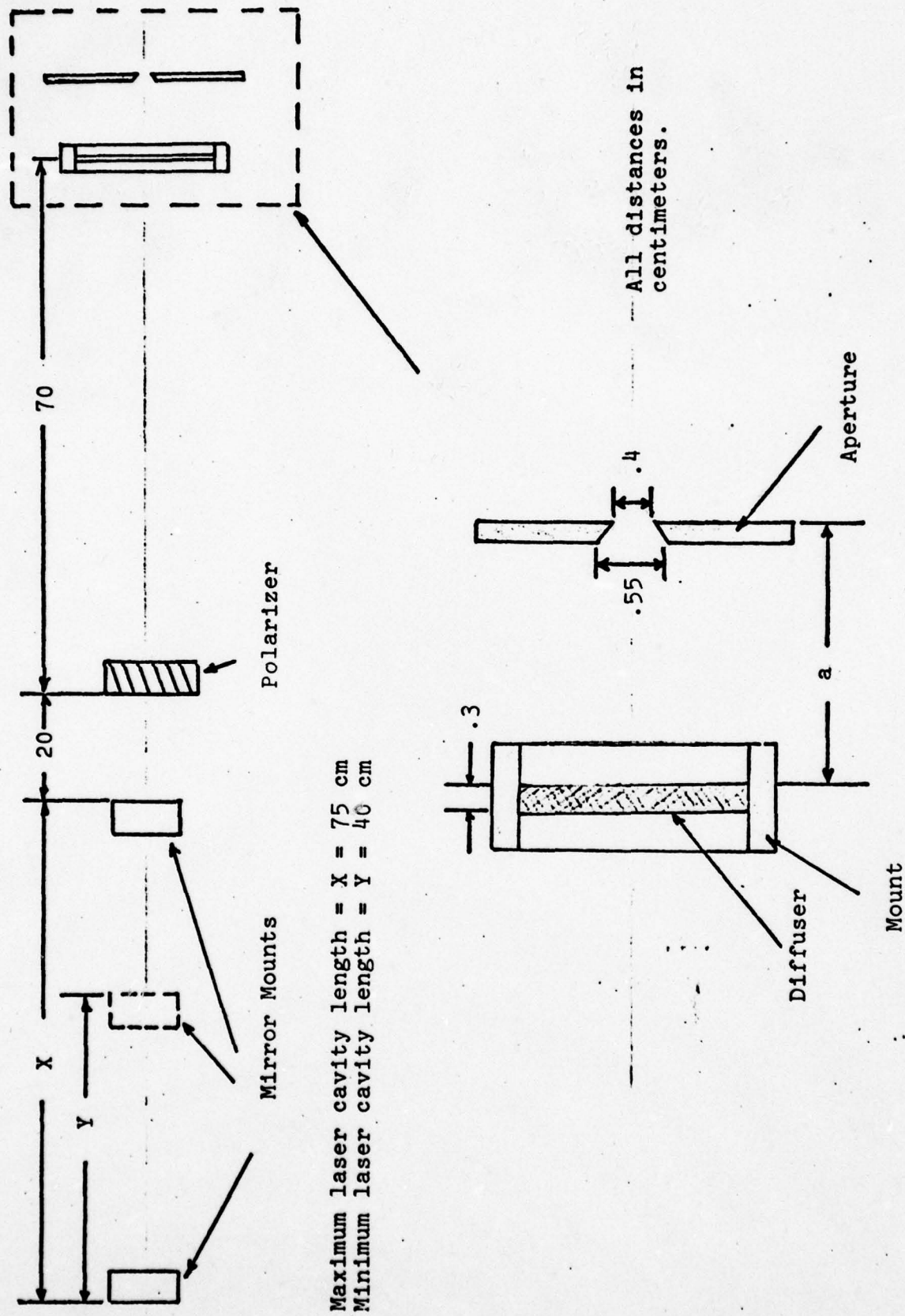
Figure 8. Experimental apparatus for laser annealing.

decreased distance, as explained.

To determine whether the energy measurements made through
the aperture were valid, a simple field of view calculation was
performed. This was necessary since the thermal detector in the
energy receiver housing was recessed, suggesting the possibility
that a portion of the energy incident on a sample mounted
immediately behind the aperture would go undetected by the
receiver. It was found that the energy meter accurately measured
the beam incident on a sample for the distance a in Figure 8 not
less than 2.7 cm. This is assuming an output laser beam of 1 cm
in diameter incident on the diffuser, resulting in infinite point
sources in a circular area 1 cm in diameter eminating from the
opposite side of the diffuser. The entire system is also assumed
aligned on center; i.e., the center of the aperture, the center
of the detector, and beam center are all in-line with each other.

Technique

The ruby laser was aligned on a daily basis with the
autocollimator. A test shot onto polaroid film was made
to assure that the HeNe aiming laser was in-line with the ruby laser
beam center. The polarizer was mounted such that the beam from the
aiming laser traversed the central portion of the split calcite crystal.
This beam was also used to center the aperture. Next, the diffuser
was put in place, with the aiming laser beam located as close
as possible to the center of the ground glass. Finally, the

Quartronix energy receiver was mounted immediately behind the
aperture, the center of the detector in-line with aperture
center.

Several test shots were then made with the polarizer in
the position of maximum transmission. Energy readings were
recorded and the PWHM measured on the oscilloscope for
each shot. These two parameters were averaged and used as a
basis for that day. Any desired energy up to the basis energy
over the aperture area could be obtained by rotating the
polarizer, while, at the same time, the pulse width remained
unchanged. The amount of rotation of the polarizer was based
on Malus' Law;

$$I' = I \cos^2 \theta \tag{2}$$

where

I' = output irradiance

I = input irradiance

θ = angle of inclination, 0° at
maximum transmission

The polarizer was equipped with a circular dial reading
0° to 359°; each 120° on the indicator represented 1°
inclination of the calcite crystal.

Unfortunately, changes in the appearance and transmission
characteristics of the diffuser were apparent after approximately
100 laser firings. Therefore, to insure reproducibility,
the glass was reground periodically. The minimal reduction in the
glass thickness due to grinding was not considered.

Analysis Equipment

A detailed description of the equipment used for luminiscence studies is beyond the scope of this work but can be found in Refs. 33 and 45.

For ellipsometry measurements, Gaertner L116 and L117 ellipsometers were used. Resistance and Hall measurements were made by Van der Pauw method. Information on equipment for Rutherford backscattering analysis was not available.

Samples

Since different types of samples were used throughout the experimental period, specific characteristics of each will be included at the time they are discussed. These include crystal orientation for virgin samples, as well as implant dose and implant energies for implanted samples. All GaAs samples used, either virgin or implanted, were of the semi-insulating type, doped with Cr. Virgin samples, whether used for analysis or subsequent ion implantation, were chemically polished.

System Accuracy and Reproducibility

The accuracy of measured laser energies reported in this work is important for comparison with the published work. The degree of reproducibility is also important so that further studies can, if desired, obtain the same results presented in the next section.

A minimum distance between aperture and diffuser was given on page 36 to insure accurate energy measurements. All

measurements made during this work were for diffuser to aperture distances either greater than or equal to this minimum distance.

The operation of the energy meter used for this experiment was based on a measured temperature differential between an ambient sensor and another sensor exposed to the laser beam. Ambient temperature in the lab was continually changing, due primarily to the heating/cooling unit for the laser head. Therefore, standard waiting time between measurements for the energy meter to zero itself could not be established. Waiting time was determined by how long it took the indicator to reach a point of small fluctuation, which was based on the judgement of the observer. Some loss of accuracy could have occurred due to failure to let the sensor reach the same degree of equilibrium before each measurement; this variation would be reflected in the standard deviation for a given set of energy measurements.

Most of the energy measurements for GaAs were made using .3J full deflection scale sensitivity, where scale divisions were 5 mJ. Accuracy of each reading for this case was $\pm$ 1mJ due to operator error, while the rated equipment accuracy was $\pm$ 3%. To get an average reading for any given day, usually five initial readings were taken. The very first laser shot of the day, after the equipment had been turned on and allowed at least 5 minutes "warm-up" time, was not recorded. Typical standard deviation for a set of measurements used to get a daily average reading was between 1-2mJ.

The major problems with reproducibility are in duplicating beam quality and laser energy. As stated earlier, the glass diffuser used in the lab was reground periodically to keep the amount of beam dispersion uniform. In cases where higher energy values were required, as with Si, a glass diffuser ground only on one side was used. Most of the reported work with GaAs was with a glass diffuser ground on both sides. Since the ground glass was not a perfect diffuser, beam quality was affected by cavity alignment. Any operator error with the auto-collimator would have caused small changes in alignment from day to day and hence a change in beam quality.

One other aid to system repreducibility is to keep the time between laser shots consistent during energy measurements and then use this same time interval between exposures to samples. This was not done in the lab becasue it was not believed the amount of change in system parameters would be great for the variable times between firing used. It is suggested that if there is a lapse of several hours between firings that a new set of energy measurements be recorded and a new daily average be established. Cavity alignment may also be necessary, particularly if the new average is much less than the old average. Again, the initial shot after not using the system for several hours or after any re-alignment should be done as a test firing only and not for any measurement purposes.

IV. RESULTS AND DISCUSSION

Laser Annealing of Si

Initial work was aimed at establishing a laser energy damage threshold in Si, followed by attempts at laser annealing ion implanted samples of this material. The first damage noted was in the form of scattered craters on the surface, observable under a microscope, for laser energies exceeding $1.1J/cm^2$. The PWHM for this energy was 23-25 nanoseconds, giving a peak power density of 44-48 MW/cm^2. This exceeds the light distortion threshold of $35MW/cm^2$ given by Khaibullin, et. al. (Ref. 25), where they also characterized damage as microscopic changes in the surface appearance. The referenced work may have been with higher power magnification equipment, and this would account somewhat for the discrepancy; they also used a laser pulse of 15-20 nanoseconds, which may have affected the surface differently than the longer pulse used in experimental work. The difference in homogeneity of their beam versus the beam in the experiment is unknown, but the authors did specify the use of "diffusing filters" to homogenize their laser beam.

Another contrast is the data given by Oak Ridge (Ref. 47) for B-implanted Si. They reported $1.1J/cm^2$ necessary to melt Si, while $1.3J/cm^2$ annealed the ion implanted material, for a 50 nanosecond pulse. The peak power of their annealing energy was $22MW/cm^2$, within the bracket given by Khaibullin, et. al.. But, the laser energy damage threshold for Si noted in the experimental work was the same as the melting threshold stated

41

by Oak Ridge, in terms of incident laser energy. It was considered that cratering might be an initial stage to melting, but higher energies only resulted in more craters, followed by gross damage, as mentioned. Melting of the Si samples would result in an uniform, undamaged appearance on the surface, with the exception of "ripples" over the irradiated area (Ref. 32). It was assumed, therefore, that the appearance of craters signified an energy density above that needed to melt the surface.

A reason for the observed behavior and contrasting data from the literature may be that the beam used in the experiment was not entirely homogeneous and contained microscopic hot spots, not observable on the polaroid film used for beam profiling. If so, it would have been impossible in the laboratory to reach the Oak Ridge annealing energy without causing some surface damage. Another discouraging consideration of the comparison is that the absorption coefficient for implanted samples in the Oak Ridge work should have been higher than the absorption coefficient for pure Si, based on earlier discussion. Therefore, their $1.3 J/cm^2$ annealing energy density figure should not only be matched but surpassed by the damage threshold in pure Si. As shown, this was not the case with the experimental work.

Rutherford backscattering analysis was done on laser irradiated, indium (In) - implanted Si. The In concentration was $10^{14}/cm^2$, implanted at 30 keV. The orientation of the Si substrate was (111), and this was used as the channeling direction for the aligned spectra. Figure 9(a) shows the backscattering spectra for a test sample of pure Si. Figure 9(b) shows the

42

spectra from an as-implanted sample. The peak near channel number 223 for the aligned spectrum in 9(b) indicates poor crystal lattice structure, which would be expected. Figures 10(a) and 10(b) show backscattering spectra from laser irradiated samples. The sample of Figure 10(a) was exposed to $.82J/cm^2$ ($33MW/cm^2$), below both the light distortion threshold of Khaibullin, et. al., and the damage threshold determined in the lab. For Figure 10(b), the incident laser energy and power were $1.2J/cm^2$ and $48MW/cm^2$, above both the aforementioned thresholds. Implantation into the Si wafer had caused a color change, making the surface cloudy gray. The areas irradiated by laser returned to the silvery-metallic look characteristic of the unimplanted portion of the wafer. Also, cratering was present in the sample exposed to the higher incident laser energy.

The Rutherford backscattering spectra from the laser irradiated samples are very close to the test sample spectra, indicating a return to crystallinity in the implant layer. In fact, the sample irradiated with higher energy shows slightly lower counts than the test sample, which means some elimination of defects present in the original substrate had taken place. Unfortunately, this analysis tells nothing about the concentration of In in the host. Therefore, no conclusions can be drawn about how much In became substitutional in the lattice. It is not clear why surface cratering on the sample exposed to the higher laser energy did not affect the backscattering spectra. The Oak Ridge researchers made no mention of damage in the form of craters. In fact, they provided electron micrograph pictures
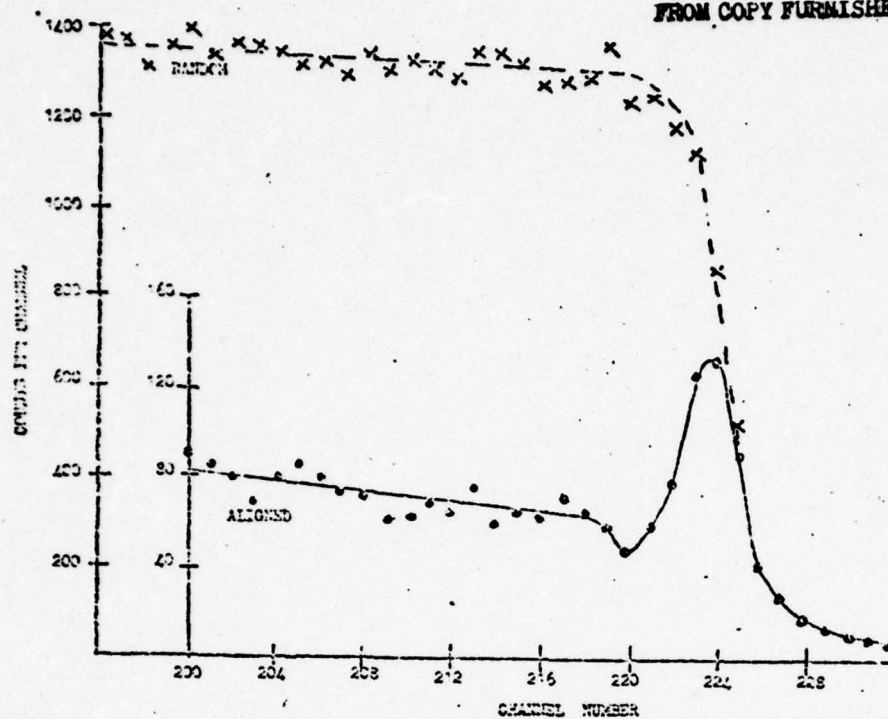
(a)
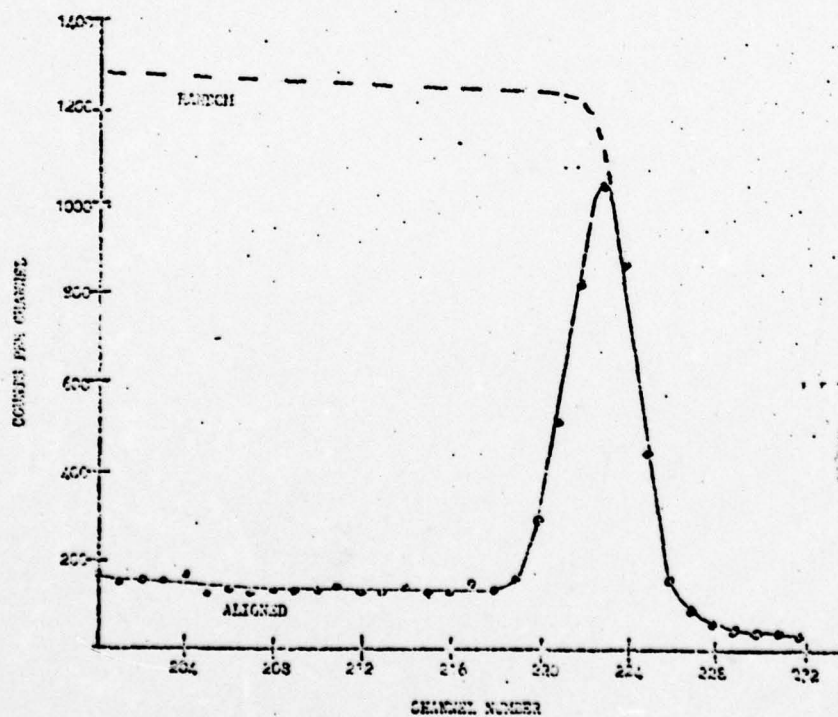
(b)

Figure 9. Rutherford backscattering spectra for (a)
pure and (b) In-implanted Si.
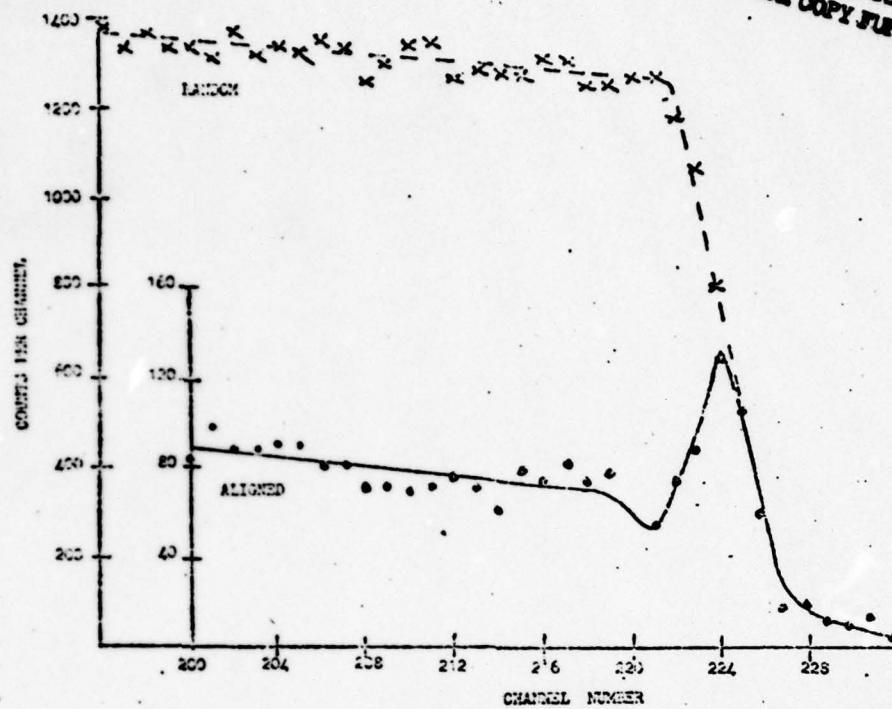
(a)
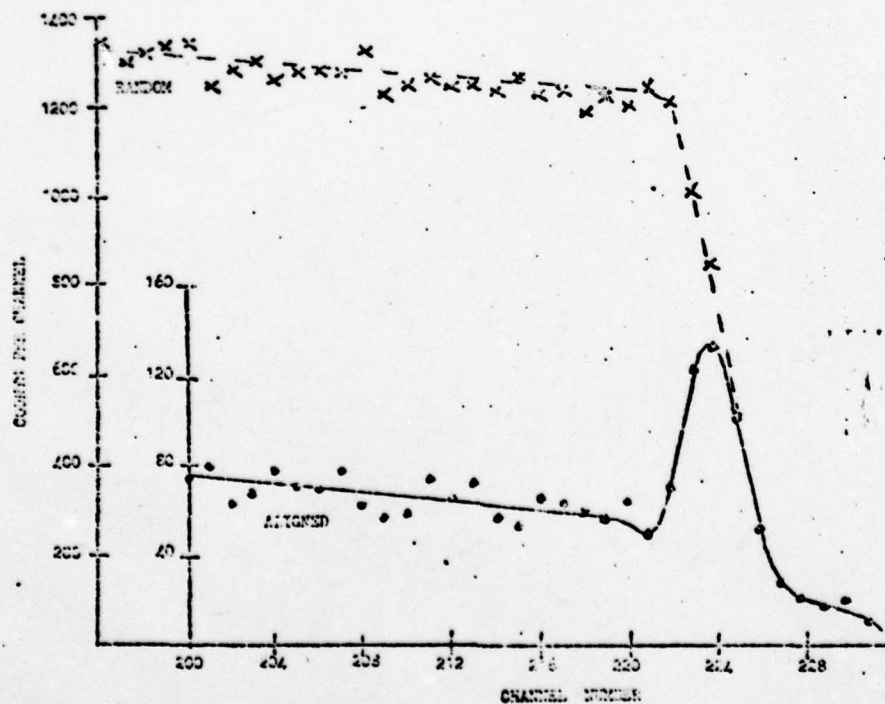
(b)

Figure 10. Rutherford backscattering spectra for
laser irradiated, In-implanted Si. The incident laser
energies were (a) .82J/cm^2 and (b) 1.2J/cm^2.

45

which showed the surface of laser annealed B-implanted Si was similar to that of pure Si. In addition, they did Rutherford backscattering analysis of the same samples (Ref. 49), showing spectra similar to Figures 9 and 10, with the exception of lower counts in their annealed sample spectra. This indicates a higher degree of anneal in their work.

The experiments with Si provided the following useful information:

(1) recrystallization of an amorphous layer occurred for laser energies of .82J/cm^2 (33MW/cm^2) and 1.2J/cm^2 (48MW/cm^2), with slightly better results from the higher laser energy,

(2) damage in the form of scattered craters, even at energies below what some published work reports to be the anneal energy for Si, indicated inhomogeneity of the laser beam, and

(3) lower laser energies than those used for Si could be used as a starting point for work with GaAs.

Laser Annealing of GaAs

Since the laser annealing energies and powers are generally 50% higher for Si than for GaAs in the published work, it was thought that damage in the form of craters in pure GaAs would not appear for energies below about .7J/cm^2. However, it was determined by experiment that scattered craters occurred for energies greater than .27J/cm^2 for a 24 nanosecond pulse (11.1MW/cm^2). Also, a color change occurred for laser energies above .14J/cm^2 (8.2MW/cm^2). It is not known why the experimental

damage threshold is so much lower than anticipated. A possible reason is that the Si samples used in the experiment were higher in purity and had less defects than the GaAs samples. Another possibility is the difference in crystal orientation; pure GaAs samples were oriented in the (100) direction, whereas Si samples had a (111) orientation, as mentioned. Also, poor beam homogeneity may have had a greater effect on GaAs than on Si. The experimental damage threshold peak power density is close to that reported by Smith (Refs. 40 and 41).

The following implants were used for laser annealing experiments with GaAs; carbon (C) (10^{13}/cm^2), Ge(10^{12}, 3x10^{13}, and 3x10^{14}/cm^2), magnesium (Mg) (10^{15}/cm^2), and Te(10^{12}, 10^{13}, and 10^{15}/cm^2). The orientation of substrates used for implantation was (100). Implantation energy for all of the above was 120keV. As a prelude to luminescence studies of laser annealed, implanted samples, pure GaAs was irradiated with varying laser energies and its luminescence spectra was compared to virgin samples, unexposed to laser light. This was used in addition to microscopic observation to search for laser related damage.

Initially, all of the luminescence spectra from pure GaAs samples irradiated at laser energies between .02J/cm^2 and 2J/cm^2 was very weak, less than spectra from samples which were implanted and unannealed (see Figure 5). Peaks attributable to damage were present but also very weak. When the probe voltage was raised high enough to penetrate through the laser irradiated sample to the point where the laser energy had decayed to a small value, the spectra was similar to the

virgin sample, but still lower. The luminescence spectra for the region near the surface of the irradiated samples indicated that laser radiation was creating damage in addition to that caused by ion implantation. Yet, the range of laser energies used in the lab on virgin GaAs samples, which all resulted in weak luminescence spectra, included all the laser annealing energies for ion implanted GaAs reported in the literature (see Appendix A).

Since it was possible that the surface of the pure GaAs samples was contaminated or had an oxide coating, a de-grease procedure was employed in the following order; (1) a rinse with TCE, (2) a rinse with Acetone, (3) a rinse with methanol, and (4) immersion in distilled water. This was followed by: (1) immersion in concentrated HCl, (2) diluting the HCl with distilled water without exposing the sample to air, and (3) blow dry. The luminescence spectra for samples prepared in this manner, subsequently exposed to the laser, were unchanged from those without the chemical preparation.

Initially, Ge-implanted and Te-implanted GaAs samples irradiated by laser also showed no luminescence. Some Te-implanted samples, however, showed color changes similar to that observed in the published experimental work as being associated with laser annealing for the same impurity density (Ref. 17). This color change was most visible for higher concentrations of implanted Te. Energies above and below the damage threshold of $.27J/cm^2$ were used, but all resulted in weak luminescent spectra. In particular, the range of laser

energies used to irradiate GaAs implanted with Te included
all energies listed in Table II.

Ellipsometry showed a decrease in absorption for Te and
Ge-implanted samples irradiated with laser energies between
$.1J/cm^2$ and $.7J/cm^2$. For an intensity of $.23J/cm^2$ on GaAs;
$Te(10^{15}/cm^2)$, the extinction coefficient, which is directly
proportional to the absorption coefficient, decreased by more
than half at a depth of $250\overset{\circ}{A}$. Electrical measurements of
resistivity and Hall effect were less encouraging, but they
did show slight improvement of laser irradiated samples over
the as-implanted samples. A significant point in comparing
luminescence with the other analysis methods in these cases
is that neither the ellipsometry or electrical measurements
showed such degradation of implant layers in GaAs irradiated
by laser as did the luminescence spectra, for comparable
incident laser energies.

Several Mg-implanted GaAs samples, after being laser
irradiated, were examined by ellipsometry and electrical
measurements only. These samples showed the best results of any
that were tested by those methods. For an incident laser energy
of $.19J/cm^2$ ($7.9MW/cm^2$), the extinction coefficient at a depth
of $500\overset{\circ}{A}$ decreased by 33%. A Mg-implanted GaAs sample which was
thermally annealed at 900°C for 20 minutes still showed a lower
extinction coefficient than the laser annealed sample. Sheet
resistivity and carrier mobility of the laser annealed sample were
$7.73x10^3\Omega/\square$ and 7.3 cm^2/volt-sec respectively, as compared to
$6.06x10^2\Omega/\square$ and 154 cm^2/volt-sec for the thermally annealed sample.

In a private correspondence with Bell labs in early
September, 1978, J. A. Golovchenko (see Ref. 15) stated
that a Ga-rich layer may be formed during laser anneal of GaAs
which he believed would cause poor results with luminescence
analysis. He inicated that Bell labs had also gotten poor
results in their work with luminescence from laser irradiated
material. Subsequent to obtaining this information, preferential
etching of pure GaAs samples exposed to laser irradiation
was done using a mixture of 1 part H_2SO_4, 1 part 30% H_2O_2, and
50 parts distilled water, all at 0°C. The rate of etch for
this solution was 200Å/minute.

Three samples of pure GaAs were shot with laser energies of
.19J/cm^2 and etched for ½ minute, 5 minutes, and 15 minutes.
All showed spectra comparable to that of the virgin material,
with the number of counts from the laser irradiated sample
spectra down by roughly a factor of two. Higher counts were
inversely proportional to etch time.

Following these improved results, Te(10^{12}/cm^2) - implanted
GaAs samples were exposed to laser energies of .19J/cm^2
(11.2MW/cm^2), .27J/cm^2(15.9MW/cm^2), .37J/cm^2 (21.8MW/cm^2),
and .76J/cm^2 (44.8MW/cm^2), followed by a 100Å etch. The
following spectra characteristics were noted; (1) all four
spectra showed improvement over those of the Te-implanted, laser
irradiated smaples observed earlier that had not been etched,
regardless of the energies used on the unetched samples,
and (2) the spectra from the sample exposed to .19J/cm^2 had the

closest resemblance to a thermally annealed sample spectra, as in Figure 6, although the laser irradiated sample spectra were still at least an order of magnitude below the thermally annealed sample spectra. Furthermore, for the four energies used, the degree of improvement shown by the spectra was inversely proprotional to the amount of incident laser energy.

Further tests on higher implant concentrations of Te in GaAs ($10^{13}/cm^2$ and $10^{15}/cm^2$) as well as Ge ($10^{13}/cm^2$) and $C(10^{13}/cm^2)$, which were exposed to laser energy of .19J/cm^2 followed by 100A etching, did not produce results comparable to those from the etched, laser irradiated sample with the Te concentration of $10^{12}/cm^2$. Use of a Si_3N_4 cap on a $C(10^{13}/cm^2)$-implanted GaAs sample showed no improvement over the spectra obtained from unetched samples. Placing a GaAs; $Te(10^{15}/cm^2)$ sample in an argon atmosphere also resulted in spectra comparable to the early work before etching.

It is not clear whether the low concentration in the $10^{12}Te/cm^2$ sample or the chemical etchant was the determing factor in the improved luminescence spectra. However, the spectra from pure GaAs samples exposed to laser irradiation with and without etching would indicate that the etchant caused the improved spectra for GaAs implanted with $10^{13}Te/cm^2$ and $10^{15}Te/cm^2$. Although not likely, since these samples were etched at different times in different solutions, the amount of material etched from the surface could have varied from sample to sample.

V. CONCLUSIONS AND RECOMMENDATIONS

Conclusions

Q-switched ruby laser irradiation of virgin GaAs results
in an attenuation of cathodoluminescence spectra in the material,
even for incident laser energies as low as $20mJ/cm^2$. Some of
this attenuation is caused by the formation of a layer on the
surface of the GaAs after ruby laser exposure; it is possible
that this is a Ga-rich layer, created by As leaving the surface
due to laser interaction.

Consistently weak luminescence spectra from ion implanted
GaAs exposed to ruby laser radiation indicate that the quality
of anneal obtained with a Q-switched ruby laser does not approach
that of thermal annealing; specifically, a lack of radiative
centers exists in the laser irradiated material which may be
due to massive defect clustering. Spectra from existing centers
is attenuated by a surface layer similar to that noted for
virgin GaAs.

It is not known whether the degree of anneal achieved
in this work was as high as the degree of anneal reported
in the published work. Laser energy densities were almost
identical in both cases, but a comparison of beam homogeneity
cannot be made. Hot spots in the laser beam used for this work
could have caused the impurity to go substitutional in only
localized areas. The result would be defect clustering,
which is one of the probable causes for the non-radiative
centers observed in this work.

The existance of radiative or non-radiative centers in
laser irradiated, ion implanted GaAs has not been specified in

the published work primarily because the methods of analysis used by the authors were less precise than luminescence. For example, light transmission and abosrption measurements only give information about the degree of crystallinity of the implanted material. Electrical measurements go a bit further; they are fair indicators of the degree of crystallinity by mobility data and of substitutionality of the impurity by conductivity data. Rutherford backscattering is more informative than either light transmission and absorption measurements or electrical mesurements becasue it tells a great deal about crystallinity and also what the density of the impurity is within the substrate. A high impurity density and good crystallinity would indicate some degree of substitutionality, although impurity clusters within the lattice would go undetected by this technique.

In examining laser irradiated, ion implanted material, it is possible for one type of analysis to show resultant characteristics comparable to thermal anneal, while another more precise technique may show other characteristics are less comparable to thermal anneal; indeed these less improved characteristics may be comparable to those from as-implanted material.

Recommendations

Improved methods of beam diffusion should be examined, followed by luminescence studies to see if beam homogeneity has an effect on the number of radiative centers created by laser exposure. Luminescience studies should also be done of ion implanted GaAs exposed to a Q-switched neodymium laser

to see if using a laser whose photon energy is below the energy gap of the material causes improved luminescence spectra. Neodymium may be more effective than ruby based on earlier discussion of high absorption at the ruby wavelength in GaAs. Also, the beam from a neodymium laser will be more homogeneous than a ruby laser beam.

A computer analysis of laser interaction with ion implanted material should be done to establish an optimum laser annealing energy. For a Q-switched laser, the optimum energy is probably at or slightly above the melting point of the ion implanted material. A computer program could, for example, generate curves similar to Figure 3 to determine the depth of melted material due to a given laser energy density. Using these curves, and knowing the implant layer depth, the laser energy necessary to melt through a given implant layer could be determined. Important parameters for such a computer program would be the index of refraction at the surface for a given laser wavelength and how this index changes during the laser pulse, and also the abosrption coefficient for a given laser wavelength throughout the implant layer, which may also change during the pulse. These parameters would have to be established by experiment, but initial computer calculations could be done using assumed average values which would remain constant for the duration of the pulse.

REFERENCE	LOCATION	HOST	IMPLANT	LASER	INCIDENT ENERGY DENSITY	INCIDENT POWER DENSITY	LENGTH OF PULSE	OPTICS	METHOD OF ANALYSIS
~	Russia	Semiinsulating	$Te(10^{15}/cm^2)$ (400keV)	Ruby, Q. S.	$.2J/cm^2$	$6.6 \times 10^6 W/cm^2$	30nsec	Diverging Lens	Light Transmission, GaAs Absorption Coefficient
?	Italy	Semiinsulating <100>	$Te(10^{15}/cm^2)$ (400keV)	Ruby, Q. S.	$.2-1.6J/cm^2$	$10-80kW/cm^2$	20nsec	None Specified	Rutherford Backscattering
17	Bell Labs	<100> N-type; P-type, .04 Ω-cm	$Te(7x10^{15}/cm^2)$ (50keV); Zn	Ruby, Q. S.; Ruby, Q. S.	$.29J/cm^2$	$2.4 \times 10^7 W/cm^2$	12nsec	Ground Glass and collimator; "	Rutherford Backscattering; Conductivity
20	Russia	Semiinsulating "Protective Film" .1μ Thick	$Te(10^{14}/cm^2)$ (35keV)	Ruby, Q. S.	$5.7x10^{-2}J/cm^2$	$1.9 \times 10^6 W/cm^2$	30nsec	Diverging Lens	Conductivity, Hall Effect
21	Russia	Semiinsulating N-type Protective Film: Si_3N_4	$Zn(5x10^{14}/cm^2)$ (40keV)	Argon-Ion	-	$<53kW/cm^2$	C. W.	Scanning Apparatus	Resistance, Hall Effect
24	Russia	N-type	$Te(3x10^{15}/cm^2)$ (35keV); $Zn(10^{16}/cm^2)$ (35keV)	Ruby, Q. S.; Ruby, Q. S.	-; "	$10^6-10^7 W/cm^2$	>10nsec; "	None Specified; "	Hall measurements Electrical; Conductivity
27	Italy	<100>	$Zn(10^{15}/cm^2)$ (400keV)	Ruby, Q. S.	-	$15-70MW/cm^2$	20-50nsec	None Specified	Rutherford Backscattering

APPENDIX A. Survey of laser anneal of GaAs.

BIBLIOGRAPHY

1. Affolter, K., et. al., "Properties of Laser Assisted Doping in Silicon," Applied Physics Letters., 33, 185(1978).

2. Antonenko, A. Kh., et. al., "Distribution of an Implanted Impurity in Silicon After Laser Annealing," Soviet Physics Semiconductors, 10, 81(1976).

3. Baeri, P., et. al., "Arsenic Diffusion in Silicon Melted by High-Power Nanosecond Laser Pulsing," Applied Physics Letters,33, 137(1978).

4. Bolotov, V. V., et. al., "Laser Annealing of Defects Responsible for Additional Optical Absorption in Ion-Irradiated Gallium Arsenide," Soviet Physics Semiconductors, 10, 338(1976).

5. Bourgoin, J. C., et. al., "Ionization Enhanced Diffusion," Journal of Chemical Physics, 59, 4042(1973).

6. Brown, W. L., et. al., "Laser Annealing of Ion-Implanted Semiconductors," In Proceedings of a conference on Rapid Solidification Processing, Nov. 13-16, 1977, Reston, Virginia.

7. Campisano, S. V., et. al., "Laser Reordering of Implanted Amorphous Layers in GaAs," Solid State Electronics, 21, 485(1978).

8. Celler, G. K., et. al., "Spatially Controlled Crystal Regrowth of Ion Implanted Silicon by Laser Irradiation," Applied Physics Letters,32, 464(1978).

9. Donnelly, J. P., "Ion Implantation in GaAs," Institute of Physics Conferences, Serial No. 33b, (1977), Chapter 4, p. 166-190.

10. Foti, G., et. al., "Amorphous-Polycrystal Transistion Induced by Laser Pulse in Self-Ion Implanted Silicon," Applied Physics, 14, 189(1977).

11. Foti, G., et. al., "Lattice Location of Te in Laser Annealed Te-Implanted Silicon," Journal of Applied Physics, 49, 2569(1978).

12. Gamo, K., et. al., "Reordering of Implanted Amorphous Layers in GaAs," Radiation Effects, 33, 85(1977).

13. Gat, A., and J. F. Gibbons, "A Laser Scanning Apparatus for Annealing of Ion-Implantation Damage in Semiconductors," Applied Physics Letters,32, 142(1978).

14. Gat, A., et. al., "Physical and Electrical Properties of Laser-Annealed Ion-Implanted Silicon," Applied Physics Letters,32, 276(1978).

56

15. Geiler, H. D., et. al., "Investigation of Laser Induced Diffusion and Annealing Processes of Arsenic-Implanted Silicon Crystals," Physical Statistics of Solids, 41, K171 (1977).

16. Gibbons, James F., "Ion Implantation in Semiconductors-Part II: Damage Production and Annealing," Proceedings of IEEE, 60, 1062(1972).

17. Golovchenko, J. A., and T. N. C. Venkatesan, "Annealing of Te-Implanted GaAs by Ruby Laser Irradiation," Applied Physics Letters, 32, 147(1978).

18. Grotzschel, R., et. al. "Laser Annealing of Arsenic Implanted Silicon," Physics Letters, 61A, 181(1977).

19. Hecht, E. and A. Zajac, Optics, Addison-Wesley Publishing Company (1976).

20. Kachurin, G. A., et. al., "Annealing of Radiation Defects by Laser Radiation Pulses," Soviet Physics Semiconductors, 9, 946(1976).

21. Kachurin, G. A., et. al., "Annealing of Implanted Layers by a Scanning Laser Beam," Soviet Physics Semiconductors, 10, 1128(1977).

22. Kachurin, G. A., and E. V. Nidaev, "Diffusion of Impurities as a result of Laser Annealing of Implanted Layers," Soviet Physics Semiconductors, 11, 350(1977).

23. Kachurin, G. A., and E. V. Nidaev, "Effectiveness of Annealing of Implanted Layers by Millisecond Laser Pulses," Soviet Physics Semiconductors, 11, 1178(1977).

24. Kachurin, G. A., et. al., "Annealing of Defects in Ion-Implanted Layers by Pulsed Laser Radiation,"

25. Khaibullin, I. B., et. al., "Some Features of Laser Annealing of Implanted Silicon Layers," Radiation Effects, 36, 225(1978).

26. Khaibullin, I. B., et. al., "Utilization Coefficient of Implanted Impurities in Silicon Layers Subjected to Subsequent Laser Annealing," Soviet Physics Semiconductors, 11, 190(1977).

27. Klimenko, A. G., et. al., "Use of Argon Laser Radiation in Restoration of Single-Crystal State of Ion-Implantation-Amorphized Silicon Surface," Soviet Journal of Quantum Electronics, 5, 1289(1976).

28. Komarov, F. F., and I. S. Tashlykov, "Formation of Defects in GaAs on Implantation of P $^+$ and Al $^+$ Ions at Various Temp," Soviet Physics Semiconductors,11, 1156(1977).

29. Kutukova, O. G. and L. N. Streltsov, "Laser Annealing of Implanted Silicon," Soviet Physics Semiconductors,10, 265(1976).

30. Larson, B. C., et. al., "Unidrectional Contraction in Boron-Implanted Laser-Annealed Silicon," Applied Physics Letters,32, 801(1978).

31. Lau, S. S., et. al., "Epitaxial Growth of Deposited Amorphous Layer by Laser Annealing," Applied Physics Letters,33, 130(1978).

32. Leamy, H. J., et. al., "Periodic Regrowth Phenomena Produced by Laser Annealing of Ion Implanted Silicon," Applied Physics Letters,32, 535(1978).

33. Lusk, Ronald L., "Cathodoluminescence on the Effects of Te Implantation and Laser Annealing in Gallium Arsenide," Unpublished Thesis, WPAFB, Ohio: AFIT(1978).

34. Mueller, J. C., et. al.,"Laser-Beam Annealing of Heavily Damaged Implanted Layers on Silicon," Applied Physics Letters,33, 287(1978).

35. Narayan, J., et. al., "A Comparative Study of Laser and Thermal Annealing of Boron-Implanted Silicon," Journal of Applied Physics, 49, 3912(1978).

36. Narayan, J., et. al, "Transmission Electron Microscope Studies of Laser and Thermally Annealed Ion Implanted Silicon," Journal of Electrochemical Society, in press, (1978).

37. Rimini, E., et. al., "Laser Pulse Energy Dependence of Annealing in Ion Implanted Si and GaAs Semiconductors," Physics Letters, 65A, 153(1978).

38. "Search and Discovery: Laser Annealing Shows Promise for Making P-N Junctions," Physics Today, July (1978).

39. Shtyrkov, E. I., et. al., "Local Laser Annealing of Implantation Doped Semiconductor Layers," Soviet Physics Semiconductors,9, 1309(1975).

40. Smith, J. Lynn, "Surface Damage of GaAs from .694- and 1.06-um Laser Radiation," Journal of Applied Physics, 43, 3399(1972).

41. Smith, J. Lynn, "Intense Laser Flux Effects on GaAs," Applied Physics, 4, 313(1974).

42. Sze, S. M., *Physics of Semiconductor Devices*, John Wiley and Sons (1969).

43. Tseng, W. F., et. al., "Grain Size Dependence in a Self-Implanted Silicon Layer on Laser Irradiation Energy Density," *Applied Physics Letters*, 32, 824(1978).

44. Vitali, G., et. al., "Surface Structure Changes by Laser Pulses in Silicon," *Physics Letters*, 63A 351(1977).

45. Walcher, James H., "Depth Resolved Cathodoluminescence of Ge-Implanted Gallium Arsenide," Unpublished Thesis, WPAFB, Ohio: AFIT(1978).

46. Walter, Martin J., "Depth - Resolved Cathodoluminescence of Carbon Implanted Gallium Arsenide," Unpublished Thesis, WPAFB, Ohio: AFIT (1977).

47. White, C. W., et. al., "Redistribution of Ion Implanted Boron Induced by Pulsed Laser Annealing," *Journal of the Electro Chemical Society*, In-Press, (1978).

48. Yariv, Amnon, *Introduction to Optical Electronics*, Holt, Rinehart, and Winston (1976).

49. Young, R. T., et. al., "Laser Annealing of Boron-Implanted Silicon," *Applied Physics Letters*, 32, 139(1978).

50. Young, R. T., and J. Narayan, "Laser Annealing of Diffusion-Induced Imperfections in Silicon," *Applied Physics Letters*, 33, 14(1978).

VITA

Robert S. Mason was born in Elizabeth, New Jersey, on September 6, 1954, the son of Frances T. and John Wesley. He was graduated in May, 1977, from the New Jersey Institute of Technology with a B.S.E.E.. He was also commissioned as a Second Lieutenant in the United States Air Force in May, 1977, and was assigned to the Air Force Institute of Technology at Wright-Patterson Air Force Base in July, 1977.

Permanent Address: 825 Monroe Avenue
                             Elizabeth, New Jersey   07201

REPORT DOCUMENTATION PAGE		READ INSTRUCTIONS BEFORE COMPLETING FORM
1. REPORT NUMBER AFIT/GEO/PH/78D-3	**2. GOVT ACCESSION NO.**	**3. RECIPIENT'S CATALOG NUMBER**
4. TITLE (and Subtitle) LASER ANNEALING OF ION IMPLANTED GALLIUM ARSENIDE		**5. TYPE OF REPORT & PERIOD COVERED** MS THESIS
		6. PERFORMING ORG. REPORT NUMBER
7. AUTHOR(s) ROBERT S. MASON 2Lt.　　USAF		**8. CONTRACT OR GRANT NUMBER(s)**
9. PERFORMING ORGANIZATION NAME AND ADDRESS Air Force Institute of Technology　(AFIT-EN) Wright-Patterson AFB, Ohio　45433		**10. PROGRAM ELEMENT, PROJECT, TASK AREA & WORK UNIT NUMBERS**
11. CONTROLLING OFFICE NAME AND ADDRESS AF Avionics Laboratory Wright-Patterson AFB OH　45433		**12. REPORT DATE** December, 1978 **13. NUMBER OF PAGES** 66
14. MONITORING AGENCY NAME & ADDRESS(if different from Controlling Office)		**15. SECURITY CLASS. (of this report)** Unclassified **15a. DECLASSIFICATION/DOWNGRADING SCHEDULE**

16. DISTRIBUTION STATEMENT (of this Report)

Approved for public release; distribution unlimited.

17. DISTRIBUTION STATEMENT (of the abstract entered in Block 20, if different from Report)

18. SUPPLEMENTARY NOTES

Approved for public release; IAW AFR 190-17

JOSEPH. P. HIPPS, MAJOR, USAF　19 Jan 79
Director of Information

19. KEY WORDS (Continue on reverse side if necessary and identify by block number)

ANNEALING
LASER ANNEALING
GALLIUM ARSENIDE
ION IMPLANTATION

20. ABSTRACT (Continue on reverse side if necessary and identify by block number)

Ion implanted GaAs, irradiated by a Q-switched ruby laser, is examined primarily by cathodoluminescence, as well as ellipsometry and electrical measurements, to evaluate the quality of laser anneal. Weak cathodoluminescence spectra from laser irradiated samples indicate far less radiative centers than in thermally annealed samples. Emitted radiation from existing centers is attenuated by the formation of a surface layer on GaAs during exposure to the ruby laser, resulting in spectra which is slightly weaker than spectra representative of the material's condition. This attenuating layer occurs in

DD $^{FORM}_{1\ JAN\ 73}$ **1473**　EDITION OF 1 NOV 65 IS OBSOLETE

(Block 20 continued)

both virgin and implanted GaAs exposed to ruby laser radiation.
Ion implanted Si, exposed to the same Q-switched ruby laser, is examined by Rutherford backscattering and indicates a return to crystallinity of the implant layer.